Prediction and attenuation of ground vibrations generated by moving trains

Shamsul Bashir[1,2,*], Aamir Rashid Chowdhary[1,2] and Nasim Akhtar[1,2]

[1]Academy of Scientific and Innovative Research, Ghaziabad 201 002, India
[2]CSIR-Central Road Research Institute, New Delhi 110 025, India

The vibration generated by underground trains and the level of vibration attenuated along the propagation path are the keys to designing mitigation measures to avoid adverse effects on the surroundings. The attenuation of vibrational energy due to geometrical and material damping was determined at the Civil Court Godown, Pune Metro, Maharashtra, India, up to 30 m. The seismic cross-hole test was used to determine the dynamic properties of the soil. It was found that the soil stratum was homogeneous and composed of basaltic rock. The total vibration level reaching the receiver was predicted for trains travelling at 80, 250 and 350 km/h, and vibration attenuation measures such as steel mass-spring systems and polyurethane mass-spring systems have been proposed.

Keywords: Mass spring systems, mitigation measures, seismic velocity, vibration attenuation.

VIBRATION through the soil caused by different sources can be a nuisance to humans, affecting their health conditions and negatively impacting the surrounding structures. The moving trains generate forces within the ground strata that propagate as ground-borne vibrations (GBVs). For underground lines, the vibration energy is transferred from the track to the tunnel wall, thereby exciting the adjacent soil medium and propagating to the surface, where it travels as surface waves. GBVs can take multiple paths from the vibration source to the receiver end. These vibrations will propagate through the ground as different waveforms, such as surface waves (*R*- and *L*-waves) with an elliptical particle motion in a vertical plane (*R* – 67%), shear waves (*S*-waves) with particle motion perpendicular to the direction of propagation (26%) and compression waves (*P*-waves) with particle motion in the direction of propagation (7%)[1,2]. The *P*- and *S*-waves spread with hemispherical wavefronts through the soil stratum, with their damping properties being inversely proportional to the distance from the source. The *R*-waves travel along the ground with a circular wavefront having a damping property that is inversely proportional to the square root of distance. Yang and Hsu[3] reported that choosing the wavenumbers appropriate for the study of loads

moving within the ground for the functions of spreading waves remains a significant problem to be considered. The properties of these waves, mainly their speed, are impacted by the characteristics of the soil stratum, particularly its stiffness and density, along with the groundwater table[4]. High frequencies are particularly damped as they travel through the soil, which leads to the mass of the vibration spectrum reaching a structure to be often below 100 Hz. Soil thus transfers track vibrations to spread an area, which is more likely to resonate with structures since the natural frequencies of most structures are below 10 Hz (refs 5–7). However, vibration transmission into structures dramatically depends on the coupling between soil and foundation. The vibrations radiating into buildings significantly rely on the soil–structure interaction[5,7,8]. Therefore, the vibrations travelling through the soil should be carefully studied for a particular location, as should the trend of wave propagation and the soil and volumetric decay of vibrations.

During subway operation, the vibration energy continuously reduces from the source to the receiver[9]. Finally, the amount of vibration that reaches the surface is 62% of that generated at the source[10]. Furthermore, ground surface vibrations (GSVs) of a tunnel built in stiff soil are often considerably low[11], and the impact of soil depth significantly depends on the excitation frequency and natural frequency of the soil strata. Based on the primary vibration frequency spectrum of the source and transmission attributes of the soil strata, GSV bounces locations vary for different sources and soil stratum conditions[12]. Eitzenberger[13] reported that when the vibration energy travels from the soil to the substructure, it is reflected at the interface because of dynamic impedances between the two mediums, resulting in a reduction in vibration level[14,15]. Zou *et al.*[16] found that the interaction between the soil and the structure significantly affects vibration transmission from the ground to the building. Typically, for a multistorey ferroconcrete building with a basement on a foundation at an overall depth of 4–5 m, a significant reduction in the vibration level between the bottom surface and the building is established for a comparatively thick layer of soft material overlaying the rocks. For foundations in contact with the rocks, coupling loss is often considered to be zero[17]. At intervals of 0–200 Hz frequency domain, the attenuation index is attenuated with an increase in underground structure stiffness.

The vibration increases as the speed of the train increases. Yao and Fang[18] examined whether factors such as the speed of the train, distance between the track and the building, density of the soil, and soil damping can significantly impact the vibrations generated by a train. If the speed of the train overpasses the R-waves within the soil stratum, a ground vibration boom occurs, with a massive enhancement of the vibration energy induced. With the increase in train speed, the critical speeds are invariably more significant than the Rayleigh wave speed, whether the soil is hard or soft, and softer soils end up at the lower overall critical speed of the system[19,20].

Therefore, before designing a mitigation measure to control these vibrations for a particular railway line, the vibration decay characteristics of the soil along that location should be known, and the possible consequences of ground vibration should also be considered[21,22]. The main objective of the present study is to predict the attenuation of vibrational energy generated by moving trains due to geometric and material damping. For trains travelling at 80, 250 and 350 km/h, the total vibration level reaching the receiver was determined and vibration attenuation mechanisms such as steel-mass spring systems (S-MSS) and polyurethane-mass spring systems (P-MSS) were suggested.

Ground vibration propagation and attenuation

Until now, various studies have been conducted on the decay characteristics of the vibration propagating through the soil. Geometric and material damping are the two major contributors that attenuate the vibration from the source to the receiver end[23].

Geometric damping

In geometric damping, the energy density of the vibrational motion (body wave) decreases as the distance (x) increases because of the increasing wavefront of the sphere-shaped body wave and hence the area of wave propagation[24]. Also, energy density decays by a factor of x^2 because the sphere surface increases with the square of the distance and the total wave energy remains constant. The radiation damping of body waves is proportional to x since the energy density (e) is directly proportional to the square of the vibration amplitude, i.e. $e \propto A^2$. Attewell and Farmer[25] found that the amplitude of body waves attenuates with x. In the case of surface waves, the energy spreads in a cylindrical and not a spherical wavefront. The amplitude of these waves decays proportionally with $\sqrt{x}$ (refs 25–27). Woods[28] formulated the geometric damping relations with the propagating wave and the source in terms of amplitude (A) and deduced that for the attenuation of body waves in the near field and far field, the amplitude is inversely proportional to x^2 and x respectively. For the attenuation of surface waves, the amplitude is inversely proportional to $\sqrt{x}$. According to

Athanasopoulos *et al*.[29], geometric damping is generally expressed as follows

$$A_s(\text{VdB}) = A_0 \left(\frac{x}{x_0} \right)^n, \tag{1}$$

where A_s (VdB) is the vibration amplitude at a distance x from the source, A_0 the amplitude at a distance of x_0 from the source and n is the coefficient of geometric attenuation. The value of n depends on the type of source, the location of the source and the type of wave. Tables 1 and 2 present the values of coefficient of geometric attenuation formulated by different authors[26,30,31]. Gotowski and Dym[26] described the geometric decay of a wave in terms of the source-dependent parameter (S). Table 1 gives the values of S for different sources. The governing equation for calculating vibration attenuation using S is as follows

$$A_s(\text{VdB}) = S \log \left(\frac{x}{x_0} \right). \tag{2}$$

Material damping

Material damping is caused by the loss of friction between the material particles and some other form of energy. This loss is the internal attenuation of energy caused due to its dissipation by deformation in a medium. From various studies conducted on vibration decay through the soils, Bornitz[32] considered both geometric and material damping and proposed a wave decay model. In his study, the vibrations generated by the drilled shafts were examined. These vibrations propagate through the soil as a point source rather than a line source. The Bornitz model can determine the attenuation of train-induced ground vibrations. The general form of the Bornitz equation[27,32,33], which provides the cumulative impacts of geometric and material damping, is as follows[27,32,33]

$$A_r = A_0 \times e^{-\alpha(r-r_0)} \left(\frac{r}{r_0} \right)^n, \tag{3}$$

where A_r is the amplitude of the wave at a distance of r from the source, A_0 the amplitude of the wave at a distance of r_0 from the source, α the vibration decay coefficient of the material and n is the geometric damping coefficient. The amount of dampening caused by material damping is influenced by the soil type and vibration frequency (f). Therefore, the coefficient of material attenuation (α m^{-1}) is represented by eq. (4)[32].

$$\alpha = \frac{\pi \eta f}{V}, \tag{4}$$

where η is the damping loss factor of the soil, f is the wave frequency and V is the wave propagation velocity. A generalized consideration of the physics of seismic wave

Table 1. Geometric attenuation coefficient (n)[26,30]

Physical source	Type of source	Location of source	Type of wave	n	S
Highway/rail line/footing/array	Line	Surface	Surface	0	0
		Surface	Body	1	20
Car into pothole/single footing	Point	Surface	Surface	0.5	10
		Surface	Body	2	40
Tunnel	Buried line	Interior	Body	0.5	10
Buried explosion	Buried point	Interior	Body	1	20

Table 2. Geometric attenuation coefficient[31]

Position	Type of wave	Observation point	n
Point source on surface	Rayleigh	Surface	0.5
Point source on surface	Body	Surface	2
Point source at depth	Body	Surface	1
Point source at depth	Body	At depth	1

Table 3. Values of α at 50 Hz (ref. 37)

Material and source	Velocity (km/s)	α (km^{-1})
Granite		
Quincy, Mass	5	0.2–0.3
Rockport, Maine	5.1	0.237
Westerly, RI	5	0.384
Basalt		
Painesdale, Mich	5.5	0.414
Diorite	5.78	0.21

transmission within the subsurface yields eq. (5) for predicting the α values.

$$\alpha = \frac{2\pi\xi f}{V_r}, \tag{5}$$

where ξ is the damping ratio of the material and V_r is the Rayleigh wave velocity. The value of α depends on the material type. Stiffer soils have low values of α. In contrast, softer soils have higher values of α, as indicated by eq. (5) that α is directly proportional to the frequency of vibration and damping ratio of the soil. However, it is inversely proportional to the Rayleigh wave velocity. Various researchers have presented the values of α for various soil types[23,28,34–36]. However, very few studies have been conducted on vibration attenuation through rocks, as various rock attenuation mechanisms are not well understood[37]. Table 3 presents the material attenuation coefficient (α) values for seismic waves having a frequency of 50 Hz.

In eqs (4) and (5), the velocity V is the Rayleigh wave velocity (V_r) because the Bornitz equation considers only the surface waves, which is the only disadvantage of this method. In the case of vibrations generated by the underground metro train, both body (interior) waves and surface waves are generated. Therefore, the effect of shear wave velocity V_s and the pressure wave velocity V_p of wave propagation

needs to be considered. V_r is slightly less than V_s (ref. 29) and eq. (6) gives the relationship between V_r and V_s.

$$V_s = \mu V_r, \tag{6}$$

where μ is a function of Poisson's ratio[23].

Methodology and research significance

The first step in selecting a metro corridor for the study is determining the highest potential for impact from GBV. The general assessment approach was employed to evaluate vibration levels at the source. The predicted values were compared to the impact criteria for general vibration evaluation to determine the probability of vibration influence[38–41]. The purpose was to establish a relatively accurate group of people and structures that will be subjected to GBV levels that exceed the threshold. Borehole data at a particular site was recorded employing the seismic cross-hole test. The soil type was explored, and consequently, vibration transmission along the path was assessed. Then the dampening of vibration due to geometric and volumetric decay through the stratum was measured. Therefore, the demand for vibration mitigation was anticipated at each chainage, and consequently, vibration control mechanisms have been proposed. With the increase in speed of the train, the vibration along the corridor also increases; hence advanced mitigation measures are needed to control it. The present study provides insights into the vibration-dampening ability of the ground with hard rocks, which directly influences the development of a mitigation measure. This study will provide guidance and is relevant to researchers for accurate vibration assessment along the propagation path and the type of mitigation measure, i.e. MSS to be adopted at varying speeds. Researchers will be able to understand in detail the considerations to be made for the future and improving the operation of the metro system.

We considered two case studies. The first case is for the low speed of the train (80 km/h), the operational speed on the Pune Metro and most of the Indian metro corridors. The second case is for higher speeds of 250 and 350 km/h. The following codes were used for evaluation: Federal Transit Administration (FTA, 2018), Research Design and Standards Organization (RDSO, 2015), ISO-2631-Part-1, 1997 and ISO-2631-Part-2, 2003 (refs 38–41).

Table 4. Dynamic properties of the soil

Compression wave velocity V_s (m/s)	Shear wave velocity V_r (m/s)	Young's modulus E (kPa)	Shear modulus G (kPa)	Poisons ratio v
3812–5333	2170–2909	2.90×10^7–5.24×10^7	1.14×10^7–2.03×10^7	0.22–0.30
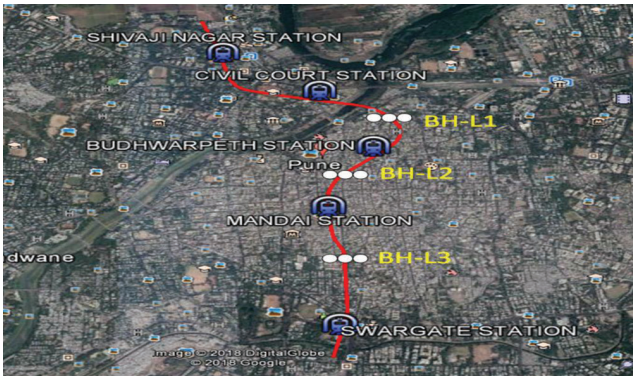
Figure 1. Map of the study site showing the location of boreholes.
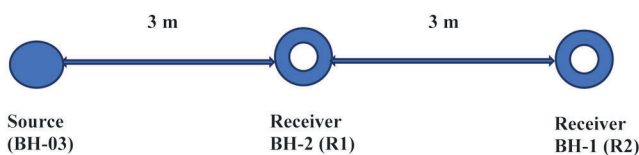
Figure 2. Seismic cross-borehole test set-up.

Field measurements

A seismic cross-hole test was conducted according to IS 13372-Part 2 (2001) to determine the attenuation of vibration amplitude due to the geometric and material damping of seismic waves. Soil properties were determined up to 30 m at the civil court in Godown, Pune Metro. Figure 1 shows the geographic positions of the seismic cross-hole measurement locations. The equipment consisted of the freedom data PC, the P–SV electromechanical borehole source (used to generate the compression and shear waves), two triaxial geophones and other accessories. The triaxial geophones were used to receive seismic waves. The freedom data PC with a cross-hole seismic system and Wingeo software (Olson Instruments) were used to record the P-SV source input and receiver output. The electromagnetic P-SV source is typically lowered to the measurement depth in a borehole and secured to the casing walls using a pneumatically activated piston in the test setup (Figure 2). It was found that the soil stratum was homogeneous basalt rock. Different parameters such as *in situ* shear and compression wave velocity, dynamic Poisson's ratio, Young's modulus and shear modulus were determined (Table 4).

The test was conducted by generating compression and shear waves travelling horizontally at a particular depth in one borehole, i.e. the source borehole. Their arrival was recorded at the same depth in two nearby boreholes, i.e.

receiving boreholes (Figure 2). After recording the travel times and travel distance at each measurement depth, wave velocities were calculated.

Five boreholes in two mutually perpendicular directions, spaced about 4 m apart at each location, were drilled using the rotary drilling technique for cross-hole seismic testing. Among these, the corner borehole (BH 03), which is at a distance of 3 m and 6 m from the receiver boreholes 2 and 1 respectively, was considered as the source borehole for generating seismic waves. The remaining four boreholes were used for lowering triaxial geophones at various depths to record *P*- and *S*-wave arrivals. The logging interval was maintained at 1.5 m by moving the source and recording the geophone in the respective boreholes step by step. The test started from the bottom of the borehole and was conducted up to 1 m depth. Each test at a particular depth was repeated thrice in the up and down directions to ensure consistency in the velocities measured. The average of three sets of velocity at each depth was considered as the expected value for a particular depth.

Data processing

The collected data were processed using the Wingeo analysis program (Olson Instruments). From the seven channels in the study, at channels 1–3, the first triaxial geophone was used, while at channels 4–6, the second triaxial geophone was used, and at channel 7 the cross-hole source trigger was used.

The arrival of the shear-wave energy is often indicated by a split in the polarization (Figure 3). The down-impact direction was recorded in magenta (Figure 3), and the corresponding shear-wave energy showed a positive break. The opposite was true for the up-impact direction. The corresponding shear wave energy in the up-direction showed a negative break.

The arrival of the compression wave energy is indicated by the first break, positive or negative, at a given depth after the trigger offset has been accounted for (Figure 4).

As outlined above, the down-hole source arrival time was corrected to zero by selecting the breaking point for each depth. Once the break time has been selected and the zero function enabled, both the up and down components should line up on zero (Figure 5). Figure 6 shows the compression and shear seismic velocities obtained from the study.

Results and discussion

According to RDSO, FTA and ISO-2631-Part 1 guidelines, a vibration level of less than 0.1 mm/s or 72 VdB is acceptable

for human comfort at a reference speed of 2.54×10^{-5} mm/s. On the other hand, vibration levels greater than 72 VdB are uncomfortable for humans. This indicates that the maximum allowable vibration limit at the ground considering human response to vibrations is 72 VdB (refs 38–40). However, according to ISO-2631-Part 2 standards, if the value of vibration exceeds 100 VdB, a crack will develop in the structure[41]. Therefore, it is necessary to determine the vibration at the
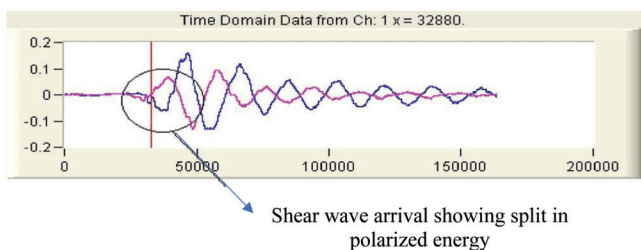

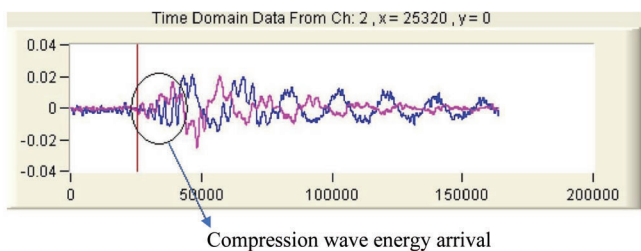**Figure 3.** Shear-wave arrival showing split in polarized energy.

Figure 4. Compression wave energy arrival.

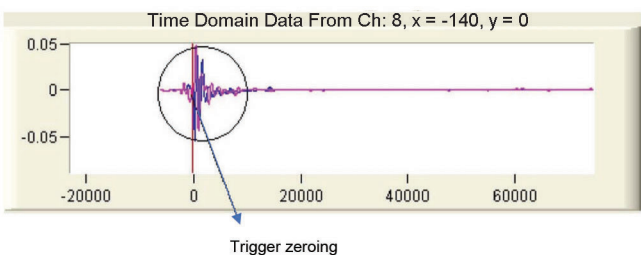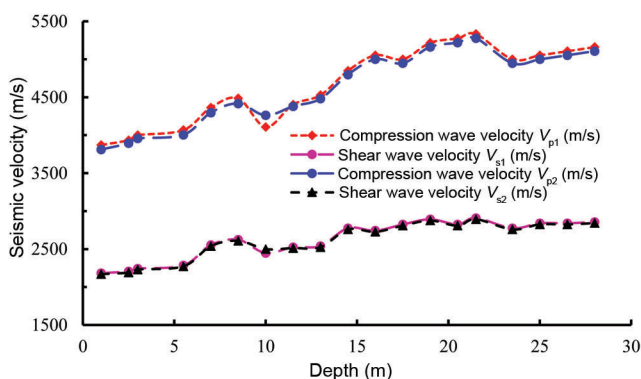**Figure 5.** Trigger zeroing.

Figure 6. Variation of seismic velocity with depth.

source, how much it gets damped along the path, and finally, which vibration attenuation system should be adopted at the source. The present study uses eq. (2) to calculate the geometric damping and eq. (3) to calculate material damping. For calculating geometric damping, the value of S has been taken as 10 VdB (Table 1) and the value of α 0.414 km^{-1} (Table 3). Table 5 provides the total amount of vibration decay along the propagation path.

Case-I: For a train speed of 80 km/h

In this study, the chainages 11,320–1,680, 12,000–12,300, 2,700–12,800, 13,400–13,960, 13,960–14,500, 14,520–15,180 and 15,180–16,400 of the Pune Metro line (north–south corridor) were taken into account. The maximum design speed of the train was 90 km/h, but the maximum operating speed was 80 km/h. The axle load of the train was 16 tonnes and an unsprung mass of 15% was considered. The maximum vibration of 92 VdB (global value) was considered for emission from a 16-tonne train with an operating speed of 80 km/h, according to the guidelines[38,39].

According to the RDSO and FTA guidelines, vibration levels must be added or subtracted based on factors such as track structure conditions, the number of building stories, etc. As a result, in the present study, a +5 VdB correction for the jointed track structure was used because the slab tracks are connected using dowel joints. Now, if the factors such as corrugation, general wear or mill scale occur on a new track, then the adjustments in vibration levels are to be taken as +5 to +15 VdB higher than the expected value. Here, the minimum increase was considered, i.e. +5 VdB.

Vibration levels are often attenuated as they are transmitted through the building. In response, resonance in the structural system, especially the floors, will generate considerable vibration amplification. Modifications for the first floor, considering a basement, are as follows: for coupling loss, –5 VdB; for the propagation of vibration energy from the basement to the first floor, an adjustment of –2 VdB; and a +6 VdB adjustment for floor amplification were adopted[38,39]. Therefore, the total adjustment was $-5 - 2 + 6 = -1$ VdB.

A total vibration of $92 + 5 + 5 - 1 = 101$ VdB will be observed at the source, considering the above modifications in vibration levels. Majority of the modifications are highly influenced by the excitation force frequency range and vibration transmission frequency dependence. It is vital to highlight that if the form of the exact vibration spectrum is not adequately examined, an improper vibration control technique may be selected, increasing the vibration levels.

From Table 4, the average shear wave velocity of 2900 m/s was taken in the study. As the shear velocity along the propagation path is very high, vibration decay is mainly due to the volumetric decay and not the soil/material damping decay (Table 5). The average path decay of vibration was considered, i.e. 10 VdB. Therefore, the vibration reaching the

Table 5. Vibration decay data along the propagation path

Depth (m)	Shear velocity (m/s)	Frequency (Hz)	Volumetric decay (VdB)	Soil/material decay (VdB) for $\alpha = 0.414$ km^{-1}	Total decay (VdB)
15	2900	50–60	7	0	7
17			8	0	8
19			8	0	8
21			8	0	8
23			9	0	9
25			9	0	9
27			10	0	10
29			10	0	10
31			10	0	10
33			10	0	10
35			11	0	11
37			11	0	11

structures was 101 – 10 = 91 VdB. So, there is a need to attenuate 91 – 72 = 19 VdB of vibration for human and structural comfort. It is to be noted that vibration on the ground floor will be 91 VdB during a single train pass-by condition, and it will be approximately 94 VdB when two trains cross simultaneously[38,39].

Case-II: For higher train speeds of 250 and 350 km/h

GBV levels fluctuate around 20 times the logarithm of the speed. This indicates that doubling the train speed increases the vibration responses by about 6 VdB. Therefore, for a speed of 180 km/h, the magnitude of vibration will be doubled for an increase of every 6 VdB, while for a speed of 350 km/h, the magnitude of vibration will be almost four times as high at the source. Equation (7) is the generalized formula used to calculate the vibration emission levels at other train speeds, in which the reference speed is taken as 80 km/h (refs 38, 39 and 41). So, for a maximum operating speed of 250 and 350 km/h, the vibration levels of 101 and 104 VdB are predicted to be generated at the source.

$$\text{VdB} = 20 \log \frac{V}{V_{\text{Ref.}}}. \tag{7}$$

After all the adjustments, same as in case-I, are applied to the vibration levels generated by a speed of 250 km/h, a total vibration emission of 101 + 5 + 5 – 1 = 110 VdB will be observed at the source. Taking the path decay of vibration as an average of 10 VdB from Table 5, the vibration reaching the structures will be 110 – 10 = 100 VdB. So, there is a need to attenuate 112 – 72 = 28 VdB of vibration for a speed of 250 km/h. Similarly, for a speed of 350 km/h, the vibration reaching the structures will be 103 VdB; so the amount of vibration to be attenuated is 103 – 72 = 31 VdB.

Proposition of mass-spring systems

The vibration-attenuating ability of the rock strata is found to be low due to their higher shear wave velocity (Table 5).

Therefore, depending on the vibration decay results along the propagation path, Table 6 presents the recommendation of MSS for vibration emission at 80, 250 and 350 km/h. At the curve portion, vibration adjustment of +5 VdB is applied due to the high dynamic interaction between the rail and wheel. To obtain a better design, ± 3 VdB can be adjusted[38,39].

For a speed of 80 km/h, the mitigation measure, i.e. discrete P-MSS with a natural frequency of 13–14 Hz and S-MSS with a natural frequency of 7–8 Hz have been suggested to attenuate the vibration of about 15–17 and 20–23 VdB respectively. Only S-MSS has been suggested for higher speeds due to high vibration emissions. Therefore, for a speed of 250 km/h, mitigation measures with a natural frequency of 6–7 and 4.5–5 Hz have been suggested to attenuate 23–28 and 31–34 VdB of vibration respectively. Similarly, for a speed of 350 km/h, mitigation measures with a natural frequency of 4–5, 5 and 6–7 Hz should be adopted to attenuate 31–36, 31 and 23–28 VdB of vibration respectively.

Conclusion

The characteristics of propagation and absorption of vibrations within the basaltic rock strata caused by train loading were examined and the following inferences have been drawn from this study:

- With increasing ground depth, the geometric decay of vibration energy increases and an average of 10 VdB is deducted from the source vibration. However, no vibration decay was observed due to material dampening.
- The vibration attenuation requirement of the system increases in direct proportion to the speed of the train. Therefore, low-frequency mitigation techniques have been proposed to reduce high-magnitude vibrations.
- Two MSS, i.e. discrete P-MSS and S-MSS have been proposed depending on the vibration emissions of the source. For vibration emissions less than 18 VdB, P-MSS and for those above 18 VdB, S-MSS are more suitable.

Table 6. Recommendations for mass spring systems (MSS) at different train speeds

Chainage (m)	Section	Rail-level depth (m)	80 km/h			250 km/h			350 km/h			
			Vibration at GL (VdB)	MSS frequency (Hz)	Mitigation (VdB)	Vibration at GL (VdB)	MSS[a] frequency (Hz)	Mitigation (VdB)	Vibration at GL (VdB)	MSS[a] frequency (Hz)	Mitigation (VdB)	Permissible limit (VdB)
11,320–11,680	Straight	15–17	91	13–14 (P*)	15–17	100	6–7	23–28	103	5	31	72
12,000–12,300	Curve	23–25	91 + 5 = 96	7–8 (S**)	20–23	100 + 5 = 105	4.5–5	31–34	103 + 5 = 108	4–5	31–36	72
12,700–12,800	Minor curve	27–29	91	13–14 (P*)	15–17	100	6–7	23–28	103	6–7	23–28	75[b]
13,400–13,960	Curve	21–24	91 + 5 = 96	7–8 (S**)	20–23	100 + 5 = 105	4.5–5	31–34	103 + 5 = 108	4–5	31–36	72
13,960–14,500	Straight	21–26	91	13–14 (P*)	15–17	100	6–7	23–28	103	5	31	72
14,520–15,180	Curve	17–21	91 + 5 = 96	7–8 (S**)	20–23	100 + 5 = 105	4.5–5	31–34	103 + 5 = 108	4–5	31–36	72
15,180–16,400	Straight	19–23	91	13–14 (P*)	15–17	100	6–7	23–28	103	5	31	72

Note: *P-MSS, **S-MSS, [a]MSS suggested for 250 and 350 km/h are S-MSS. [b]75 VdB is the vibration limit for daytime.

- The vibration intensity increases by nearly +5 VdB along the curve of the track structure system due to the significant dynamic interaction between the rail and wheel. As a result, at the curves, S-MSS is observed to be more suitable.

Conflict of interest: The authors declare no potential conflict of interest

1. Miller, G. F., Pursey, H. and Bullard, E. C., On the partition of energy between elastic waves in a semi-infinite solid. *Proc. R. Soc. A*, 1955, **233**(1192), 55–69; https://doi.org/10.1098/rspa.1955.0245.

2. Kouroussisa, G., Connolly, D. P. and Verlinden, O., Railway-induced ground vibrations – a review of vehicle effects. *Int. J. Rail Transp.*, 2014, **2**(2), 69–110; https://doi.org/10.1080/23248378.2014.897791.

3. Yang, Y. B. and Hsu, H. L., A review of researches on ground-borne vibrations due to moving trains via underground tunnels. *Adv. Struct. Eng.*, 2006, **9**(3), 377–392; https://doi.org/10.1260/136943-306777641887.

4. UIC, Railway induced vibration, state of the art report. International Union of Railways, 2017, pp. 1–82.

5. Eitzenberg, A., *Train Induced Vibrations in Tunnels: A Review*, Luleå University of Technology, Luleå, Sweden, 2008, pp. 1–90.

6. Connolly, D. P., Kouroussis, G., Woodward, P. K., Costa, P. A., Verlinden, O. and Forde M. C., Field testing and analysis of high-speed rail vibrations. *Soil Dyn. Earthq. Eng.*, 2014, **67**, 102–118; https://doi.org/10.1016/j.soildyn.2014.08.013.

7. Ribes-Llario, F., Marzal, S., Zamorano, C. and Real, J., Numerical modelling of building vibrations due to railway traffic: analysis of the mitigation capacity of a wave barrier. *Shock Vibr.*, article ID 4813274, 2017, pp. 1–11; https://doi.org/10.1155/2017/4813274.

8. Remington, P. J., Kurzweil, L. G. and Towers, D. A., Low frequency noise and vibrations from trains. In *Transportation Noise Reference Book* (ed. Nelson, P. M.), Boston, Butterworth, London UK, 1987.

9. Yang, Y. B., Hung, H. H. and Hsu, L. C., Ground vibrations due to underground trains considering soil-tunnel interaction. *Interact. Multiscale Mech.*, 2007, **1**(1), 157–175; https://doi.org/10.12989/imm.2008.1.1.157.

10. Shi, W., Miao, L., Luo, J. and Zhang, H., The influence of the track parameters on vibration characteristics of subway tunnel. *Shock Vibr.*, article ID 2506909, 2018, pp. 1–12; https://doi.org/10.1155/2018/2506909.

11. Yang, Y. B. and Hung, H. H., Soil vibrations caused by underground moving trains. *J. Geotech. Geoenviron. Eng.*, 2008, **134**(11), 1633–1644; https://doi.org/10.1061/ (ASCE) 1090-0241.

12. Wang, W., Liu, W., Sun, N. and Ma, M., Study on vibration bounce area caused by metro-based on the pulse impact experiment. In *Series: Advances in Intelligent Systems Research*, Atlantis Press, Springer Nature, 2012, pp. 0839–0843; https://doi.org/10.2991/emeit.2012.18.

13. Eitzenberger, A., Inventory of geomechanical phenomena related to train-induced vibrations from tunnels. Doctoral Dissertation, Luleå University of Technology, Sweden, 2008, pp. 1–84.

14. Kouroussis, G., Parys, L. V., Conti, C. and Verlinden, O., Prediction of ground vibrations induced by urban railway traffic: an analysis of the coupling assumptions between vehicle, track, soil and building. *Int. J. Acoust. Vib.*, 2013, **18**(4), 163–172; 10.20855/ijav.2013.18.4330.

15. Shi, W., Bai, L. and Han, J., Subway-induced vibration measurement and evaluation of the structure on a construction site at curved section of metro line. *Shock Vibr.*, article ID 5763101, 2018, 1–18; https://doi.org/10.1155/2018/5763101.

16. Zou, C., Wang, Y. and Tao, Z., Train-induced building vibration and radiated noise by considering soil properties. *Sustainability*, 2020, **12**, 1–17; https://doi:10.3390/su12030937.

17. Vogiatzis, K. and Mouzakis, H., Ground-borne noise and vibration transmitted from subway networks to multi-storey reinforced concrete buildings. *Transport*, 2018, **33**(2), 446–453; https://doi.org/10.3846/16484142.2017.1347895.

18. Yao, J. and Fang, L., Building vibration prediction induced by moving train with random forest. *J. Adv. Transp.*, Article ID 6642071, 2021, 1–13; https://doi.org/10.1155/2021/6642071.

19. Hu, J., Bian, X. and Jiang, J., Critical velocity of high-speed train running on soft soil and induced dynamic soil response. *Proc. Eng.*, 2016, **143**, 1034–1042; doi:10.1016/j.proeng.2016.06.102.

20. Krylov, V. V., *Ground Vibrations from High-Speed Railways Prediction and Mitigation*, ICE Publishing, London, UK, 2019, p. 359; ISBN: 978-0-7277-6379-2.

21. Krylov, V. V., Ground vibration boom from high-speed trains. *J. Low Freq. Noise, Vib. Active Control*, 1999, **18**(4), 207–218.

22. Krylov, V. V., *Noise and Vibration from High-Speed Trains*, Thomas Telford, London, 2001.

23. Richart, F. E., Hall, J. R. and Woods, R. D., *Vibrations of Soils and Foundations*, Prentice-Hall, New Jersey, USA, 1970, pp. 1–216.
24. Ewing, W. M., Jardetzky, W. S. and Press, F., *Elastic Waves in Layered Media*, McGraw-Hill Book Co, New York, USA, 1957.
25. Attewell, P. B. and Farmer, I. W., Attenuation of ground vibrations from pile driving. *Ground Eng.*, 1973, **6**(4), 26–29; http://worldcat.org/issn/00174653.
26. Gotowski, T. G. and Dym, C. L., Propagation of ground vibration: a review. *J. Sound Vibr.*, 1976, **49**(2), 79–93; https://doi.org/10.1016/0022-460X (76)90495-8.
27. Das, B. M., *Fundamentals of Soil Dynamics*, Elsevier Science Publishing Co, New York, USA, 1983, pp. 1–399.
28. Woods, R. D., Screening of surface waves in soils. *J. Soil Mech. Found. Div., ASCE*, 1968, **94**, 951–979.
29. Athanasopoulos, G. A., Pelekis, P. C. and Anagnostopoulos, G. A., Effect of soil stiffness in the attenuation of Rayleigh-wave motions from field measurements. *Soil Dyn. Earthq. Eng.*, 2000, **19**(4), 277–288; https://doi.org/10.1016/S0267-7261 (00)00009-9.
30. Kim, D. S. and Lee, J. S., Propagation and attenuation characteristics of various ground vibrations. *Soil Dyn. Earthq. Eng.*, 2000, **19**(2), 115–126; https://doi.org/10.1016/S0267-7261 (00)00002-6.
31. Amick, H. and Gendreau, M., Construction vibrations and their impact on vibration-sensitive facilities. In *Construction Congress VI*, ASCE Library, Orlando, Florida, 2000; https://doi.org/10.1061/40475 (278)80.
32. Bornitz, G., *Über die Ausbreitung der von Grobkolbenmaschinen erzeugten Bodenschwingungen in die Tiefe* (*Propagation of the Ground Vibrations Generated by Large Piston Machines into the Depths*), Springer, Berlin, Germany, 1931.
33. Mintrop, L., Uber die Ausbreitung der von den Massendrucken einer Grossasmaschine erzeugten Bodenschwingungen (Spread of the ground vibrations generated by the mass pressures of a large gas engine). Ph.D. Dissertation, University of Gottingen, Germany, 1911.
34. Kushida, H., *Engineering of Environmental Vibration*, Rikodosho, Tokyo, Japan, 1997.
35. Peng, S. M., Propagation and screening of Rayleigh waves in clay. Master's Engineering thesis, Asian Institute of Technology, Bangkok, Thailand, 1972.
36. Barkan, D. D., *Dynamics of Bases and Foundations*, McGraw Hill, Book Company, 1962, vol. 42, p. 434.
37. Dobrin, M. B. and Savit, C. H., *Introduction to Geophysical Prospecting, Fourth Edition*, McGraw-Hill Book Company, 1988, pp. 39–48.
38. Federal Transit Administration, *Transit Noise and Vibration Impact Assessment Manual*, FTA Report No. 0123, National Transportation Systems Center, US Department of Transportation, 2018.
39. Metro Rail Transit System, Guidelines for noise and vibrations. CT-38, Track Design Directorate, Research Designs and Standards Organisation, ISO-9001, Ministry of Railways, Government of India, New Delhi, 2015.
40. ISO-2631-Part-1, Mechanical vibration and shock–evaluation of human exposure to whole-body vibration – Part 1: general requirements, 1997, p. 31.
41. ISO-2631-Part-2, Mechanical vibration and shock – evaluation of human exposure to whole-body vibration – Part 2: Vibration in buildings (1 Hz to 80 Hz), 2003, p. 11.